# Solar prominences

Duncan H. Mackay


| | |
|---|---|
| Date of deposit | 10 03 2021 |
| Document version | Author's accepted manuscript |
| Access rights | Copyright © 2021 Oxford University Press. This work has been made available online in accordance with publisher policies or with permission. Permission for further reuse of this content should be sought from the publisher or the rights holder. This is the author created accepted manuscript following peer review and may differ slightly from the final published version. |
| Citation for published version | Mackay, DH 2021, Solar prominences. in Oxford Research Encyclopedia of Physics. Oxford University Press. |
| Link to published version | https://doi.org/10.1093/acrefore/9780190871994.013.17 |

Full metadata for this item is available in St Andrews Research Repository at: https://research-repository.st-andrews.ac.uk/

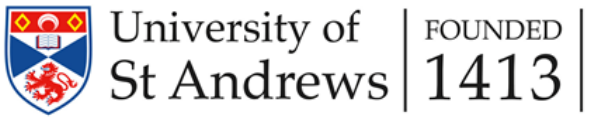

# Solar Prominences

**Article Summary and Keywords**

Solar prominences (or filaments) are cool dense regions of plasma that exist within the solar corona. Their existence is due to magnetic fields which support the dense plasma against gravity and insulate it from the surrounding hot coronal plasma. They can be found across all latitudes on the Sun where their physical dimensions span a wide range of sizes (length ~ 60-600 Mm, height ~ 10-100 Mm and width ~ 4-10 Mm). Their lifetime can be as long as a solar rotation (27 days), at the end of which they often erupt to initiate Coronal Mass Ejections.

When viewed at the highest spatial resolution, solar prominences are found to be composed of many thin co-aligned threads or vertical sheets. Within these structures, both horizontal and vertical motions of up to 10-20kms$^{-1}$ are observed, along with a wide variety of oscillations. At the present time, a lack of detailed observations of filament formation gives rise to a wide variety of theoretical models of this process. These models aim to explain both the formation of the prominence's strongly sheared and highly non-potential magnetic field along with the origin of the dense plasma. Prominences also exhibit a large-scale hemispheric pattern such that "dextral" prominences containing negative magnetic helicity dominate in the northern hemisphere, while "sinistral" prominences containing positive helicity dominate in the south. Understanding this pattern is essential to understanding the build-up and release of free magnetic energy and helicity on the Sun. Future theoretical studies will have to be tightly coordinated with observations conducted at multiple wavelengths (i.e. energy levels) in order to unravel the secrets of these objects.

Keywords: Sun, prominences, filaments, filament channel, magnetic fields, solar corona, magnetohydrodynamics, solar chromosphere.

## 1. Introduction

Solar prominences (or filaments) exist within the solar corona and can be described as locations of cool, dense plasma that are located in a much hotter and rarer environment. Prominences or filaments are typically 100 times denser and 100 times cooler than the coronal plasma that surrounds them. The terms prominence or filament refer to the same solar phenomenon (Hale, 1903; Deslandres, 1910) where the prominence is observed at the solar limb (Figure 1a) often seen in Hα emission, while a filament is seen on the solar disk in absorption of Hα (Figure 1b). Throughout this article the term prominence or filament will be used interchangeably depending on the most appropriate choice. During periods of high sunspot activity, solar filaments are found broadly spaced from equatorial to polar latitudes (Figure 1c). They are an integral part of the lower solar corona.

While they occur frequently, basic physics tells us that, under the effect of gravity, prominences should fall down to the solar surface and through thermal conduction they should heat up. Surprisingly, these objects are known to be globally stable with a lifetime that may be longer than a solar rotation (~27 days). Although they can exist in a stable configuration for a long time, they exhibit rapidly evolving small-scale structures (~100km) and a wide range of flows and oscillations. Both filaments and prominences frequently erupt outwards from the Sun and can be ejected into interplanetary space, where they and their surrounding magnetic field become a coronal mass ejection (CME) which can directly affect the Earth and lead to Space

Weather. Due to their long duration and importance for Space Weather, solar prominences are an active area of research. Key questions relating to their origin, structure, stable evolution and their eruption remain unanswered. Since the determination of their physical properties is mostly carried out through remote-sensing observations, a knowledge of radiative-transfer processes (Heinzel, 2015) in conjunction with plasma properties is important. The scientific investigation of solar prominences therefore spans many areas of research, ranging from observational techniques (imaging, spectroscopy and polarimetry), to theoretical studies (atomic physics and magnetohydrodynamics (MHD, E Priest, Oxford article). Through these distinct but complementary techniques, the lifecycle of solar prominences from birth to decay can be followed. This article describes our current understanding.

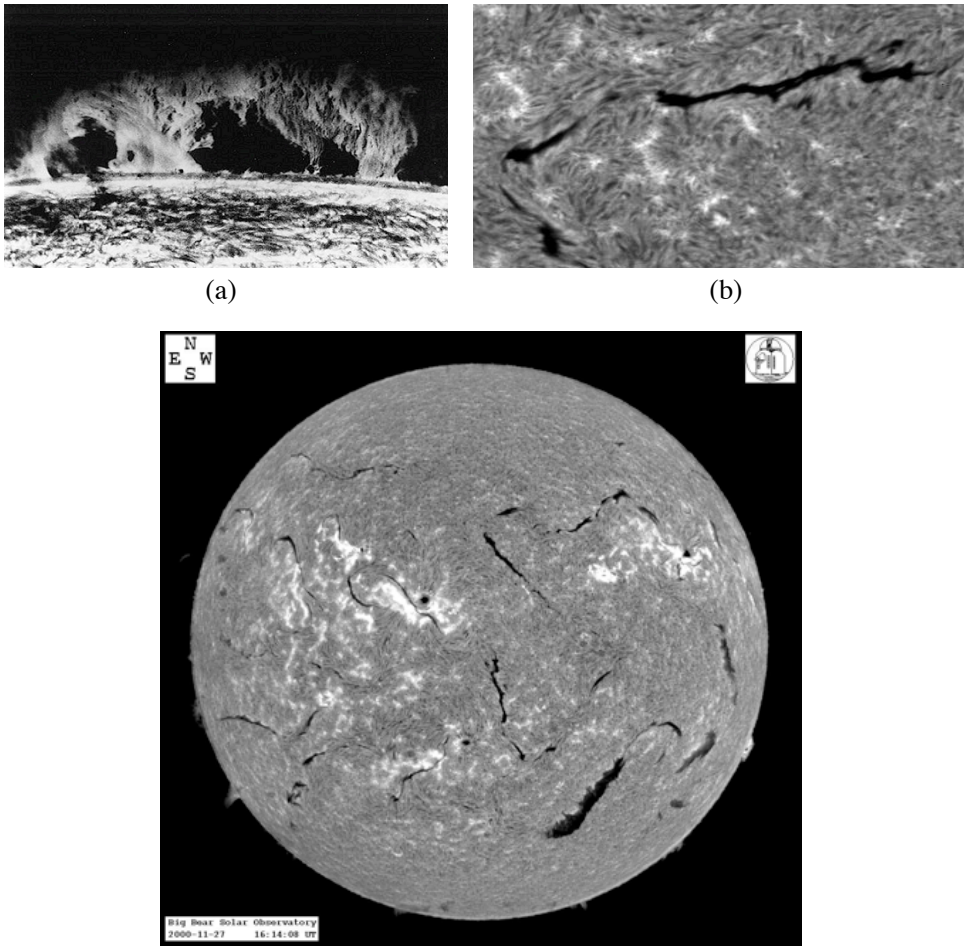


(a) (b)

(c)

Figure 1: Examples of (a) a solar prominence in Hα at the limb, (b) a solar filament in Hα on the disk and (c) full disk Hα image showing solar filaments over many latitudes. Credit: Big Bear Solar Observatory.

## 2. Historical Observations to Present Day Science

Prior to the invention of the spectroscope, solar prominences could only be observed during solar eclipses when the intense radiation from the disk of the Sun is blocked by the Moon. This allowed the faint light from the Sun's corona to be seen. One of the earliest recorded observations of prominences dates from the eclipse of 1239 where Muratori reported seeing a "burning hole in the corona". Many such additional cases were documented over the next five centuries, with solar prominences described as "burning holes", "red flames" or even as clouds or mountains on the Moon (Vassenius, 1933). Whilst the early records of prominences were documented through drawings, a significant step forward was made in 1860 with the invention of photography. This allowed the main morphological properties of prominences to be characterised and permanent records made. During the solar eclipse of July 28$^{th}$ 1851, the first recorded case of an erupting prominence was documented by Airy. In the 1860's, prominences were viewed through a spectroscope set to H$\alpha$, which confirmed their gas nature through the presence of hydrogen emission lines. This discovery led to the invention of the spectroheliograph by Hale and Deslandre in the 1890's. The first spectroscopic observations of prominences identified an unknown spectral line, which was later found to be due to the then unknown element of Helium.

The invention of the birefringent filter and coronagraph in the 1930's by Bernard Lyot revolutionised the investigation of solar prominences and the corona. Using a Lyot type H$\alpha$ filter and a 16″ chronograph, Dunn (1960, 1965) showed that solar prominences were composed of many fine scale threads around 300km wide. Surprisingly these threads were not static, but rather exhibited both upward and downward motions in the range of 5-10 kms$^{-1}$. These observations set a new standard for the detection of small-structures and dynamic motions in solar prominences.

With the invention of the magnetograph, Babcock and Babcock (1955) determined that solar filaments exhibited a close relationship to the underlying magnetic field in the solar photosphere. They found that filaments lie above polarity inversion lines that separate areas of positive and negative magnetic fields. Therefore, filaments formed at locations where the vertical component of the field is zero. Using this as stimulus, Kippenhahn and Schluter (1957) developed the first fully accepted magnetic field model of solar prominences (see also Kuperus and Raadu, 1974).

With the identification that magnetic fields are fundamental to the existence of solar prominences, efforts were then undertaken to directly measure their magnetic fields at the solar limb. The first direct measurements were made using Zeeman splitting in the H$\beta$ line (Zirin & Severny, 1961), which found field strengths in active region prominences of around 200G. The modern era of magnetic-field measurements in prominences through polarimetry was started in the 1970's at the Pic-du-Midi observatory, where the Hanle effect was used to measure weak (on the order of 10 G) magnetic fields in quiescent prominences (Leroy et al., 1977; Sahal-Brechot et al., 1977; López-Ariste 2015).

Since the 1970s, the modern era of solar-prominence research has been carried out through a wide variety of ground- (Dutch Open Telescope, Dunn Solar Telescope, Swedish Solar Telescope, THEMIS and the New Solar Telescope at Big Bear Solar Observatory) and space-(SoHO, HINODE, TRACE, STEREO, SDO and IRIS) based observatories[1]. In particular, with

[1] Many online data sets exist where catalogues of filaments can be found at http://www.helioviewer.org

space-based instruments, solar prominences may be studied in non-visible wavelengths such as UV and EUV that are blocked by the Earth's atmosphere. The results described in the following sections are derived from both ground- and space-based instruments, along with theoretical studies.

## 3. Basic Properties

Solar prominences may be observed across a wide variety of wavelengths. These wavelengths extend from visible light to the non-visible parts of the electromagnetic spectrum (Radio, UV and EUV, see Heinzel et al. 2015). While solar prominences have a multi-thermal nature, the most dense, central part of the prominence has a temperature of between 6000-10000K. This central part is visible to the naked eye and has a dark-red colour (6562.8A, Hα). The basic properties of solar prominences cover a wide range of spatial and temporal scales and are summarised in Table 1, where the thermodynamic properties have been determined using spectral observations and radiative-transfer modelling (Labrosse et al. 2010).

| Property | Range |
|---|---|
| **Density** | $10^{10}$-$10^{11}$cm$^{-3}$ |
| **Pressure** | 0.1 – 0.01 dym cm$^{-3}$ |
| **Core Temperature** | 8-10,000K |
| **Length** | 60-600 Mm |
| **Height** | 10-100 Mm |
| **Width** | 4-10 Mm |
| **Lifetime** | 1-30 days |
| **Magnetic Field Strength** | 3-30G |
| **Plasma Beta (β)** | 0.01~0.1 |

Table 1: Typical Physical Properties of Solar Prominences

While filaments may be found at all latitudes on the Sun, they always form above Polarity Inversion Lines (PILs) in the photosphere, where the radial component of the magnetic field is zero. The existence of a PIL is a necessary, but not sufficient condition for a filament. For a filament to exist there must also be a "filament channel" in the chromosphere (see Figure 2a for an illustration). Filament channels are the fundamental magnetic environment for the formation and existence of filaments (Martres et al., 1966; Gaizauskas, 1998). They are regions of the chromosphere, often observed in Hα, where on either side of the channel, fibrils are aligned parallel to the PIL but anti-parallel to one-another. These fibrils outline the local direction of the magnetic field in the chromosphere and show that the field is mainly horizontal. In addition, the anti-parallel alignment indicates that the magnetic field in the channel points in the same direction on either side (Foukal, 1971a, 1971b). These horizontal magnetic fields support the dense plasma against gravity through the Lorentz force (Figure 2b) and also insulate the cool material from the surrounding hot corona (Figure 2c), since thermal conduction across the field is negligible compared to that along the field. Filament channels are locations of strongly sheared magnetic fields, where a significant amount of free magnetic energy can be stored. Direct magnetic-field measurements have confirmed the existence of this horizontal magnetic field at coronal heights (Hyder, 1965; Rust, 1967; Leroy et al., 1983; Leroy, 1989, see Tandberg-Hanssen, 1995 for a review). Filament channels are more fundamental than the filaments that form within them, since a single channel may survive a succession of filament

formations and eruptions. In recent years, using SDO observations in the Fe XII line at 193 Å, Sheeley et al. 2013 showed the extension of filament channels into the corona through the systematic orientation of coronal cells.

When solar filaments are viewed at high resolution in Hα on the solar disk, they can be seen to be composed of three distinct structural elements: a spine, barbs and two ends. The spine extends horizontally along the top of the filament, following the path of the filament channel. It may be continuous or exhibit multiple breaks. The ends of a filament are the two extreme parts that bend down to the photosphere.

Barbs are structures that project out from the side of filaments and extend down to the chromosphere (Figure 1b). When viewed from above, they may be classified as either "right-bearing" or "left- bearing", depending on the acute angle that they make to the filament spine. Barbs are highly inclined structures that are often found to terminate close to minority polarity magnetic fields on either side of the PIL (Martin & Echols, 1994). Even though the vertical extent of the barbs is much greater than the local gravitational scale height of the plasma (200km), speeds much lower than the free-fall speed are commonly observed. Therefore, the plasma in the barb must be supported against gravity by external forces and cannot be a static field-aligned structure. One possible explanation for this support is given by the model of Aulanier and Demoulin (1998). In this model, barbs are produced by a series of vertically nested magnetic dips that are produced by minority polarity magnetic fields in the photosphere on either side of the PIL. While this model produces a natural explanation of barbs, along with their right- and left-bearing nature, it does not fit the observations of Zirker et al. (1998a) who observed both up-flows and downflows simultaneously in the same barb (Lin et al., 2003; Alexander et al., 2013). These counter-flows, with speeds in the range 5-10kms$^{-1}$ were interpreted to be flows parallel to the magnetic field in the barb. The observations indicated that the magnetic field was vertical in the barb and not horizontal as in the Aulanier and Demoulin model. To consider the support of material in a vertical magnetic field, Pesceseli and Engvold (2000) put forward an alternative model in which the barb was supported by damped high-frequency MHD waves countering gravity.

To determine if the magnetic field in barbs is mainly vertical or horizontal, López Ariste et al. (2006) used polarimetric measurements to investigate the properties of the magnetic field at the photospheric level around a barb. The measurements showed that the field at the photosphere was of inverse polarity and therefore supported the Aulanier and Demoulin (1998) model. To date there are still many unanswered questions regarding the properties and relationship of the plasma and magnetic field in barbs; new high-resolution observations including polarimetric measurements are required to answer these questions.

When an East-West-orientated quiescent prominence is observed at the limb in coronal white light, the observations show a "cavity" that lies around the prominence. The cavity separates the prominence from the surrounding coronal magnetic field and has reduced intensity compared to neighbouring regions of the corona. Measurements by Fuller et al. (2008) indicate that the plasma density within a cavity is approximately 30% less than in the surrounding coronal region. As a consequence, cavities appear darker and often extend to more than twice the height and width of the prominence. Low and Hundhausen (1995) explained the nature of the cavity as the extended flux rope that supports the mass of the filament, while the papers of Gibson (2010) and Gibson (2014) give a review of 3D models of prominence cavities. The true nature of cavities is not fully understood, but Berger et al. (2012) propose that cavities play a role in prominence formation.

The most direct method to measure the magnetic field in prominences is to use spectro-polarmetric data and inversion techniques (Paletou & Aulanier, 2003; Paletou, 2008; Lopez-Ariste & Aulanier, 2007). In the 1970's and 80s, many studies were carried out at the Pic du Midi observatory in France and at Sacramento Peak in the US (see review by Leroy, 1989). These early measurements deduced that in quiescent prominences, the magnetic field strength is between 3-15G, mainly horizontal and makes an angle of approximately 40 degrees to its long axis (Bommier & Leroy 1998). In addition, the field strength increases with height, confirming the presence of magnetic dips. The measurements also showed that the magnetic field in prominences is of "inverse polarity" (i.e. it passes over the PIL from negative to positive polarity). In recent years, a number of studies have been carried out using the Hanle-effect diagnostic. In particular, Casini et al. (2003) made the first vector-field magnetic map inside a prominence and showed that the field is not uniform, with localised patches of strong fields up to 80G.

## 4. Classification Schemes

Historically a number of classification schemes have been developed to explain the wide range of formation locations, dynamic properties and morphology of both solar filaments and prominences. These schemes have helped develop our understanding of filaments and prominences. A review of these classification schemes can be found in Engvold (2015).

One of the most commonly used classification schemes separates filaments into one of three types based on the nature of the magnetic environment in which they form: Active Region Filaments (ARF), Intermediate Filaments (IF) and Quiescent Filaments (QF). The characteristic features of these are:

- Active Region Filaments (ARF): Filaments that form at sunspot latitudes within sunspot activity nests that usually contain multiple pairs of sunspots. ARF are small thin structures that are short lived and have a lifetime of minutes to days. They frequently erupt, where their number varies in line with the solar cycle.

- Intermediate Filaments (IF): Filaments that form along the border of active regions and weaker background magnetic fields. As they border active regions, they form at active latitudes but have properties closer to those of Quiescent Filaments.

- Quiescent Filaments (QF): These filaments form in quiet Sun regions and can be found across all latitudes of the Sun. Their physical extent spans the full range of values given in Table 1. Whilst their global structure is very stable, high-resolution observations indicate that they are comprised of numerous small-scale threads, where these threads sometimes take the form of thin vertical sheets. The origin of these vertical sheets is yet to be explained, as direct magnetic-field measurements show that the field within them is horizontal.

An alternative classification scheme was put forward by Tang (1987) and later extended by Mackay et al. (2008). This scheme classifies filaments relative to the origin and evolution of the PILs above which the filaments form. Therefore, it considers both the origin and history of the magnetic interactions which lead to the formation of the filament. Mackay et al. (2008) found that over 80% of filaments form above PILs that are external to any single magnetic

bipole and therefore require the interaction of two or more bipoles. This indicates that convergence of magnetic flux and reconfiguration of the coronal field play a key role in the formation of filament channels.

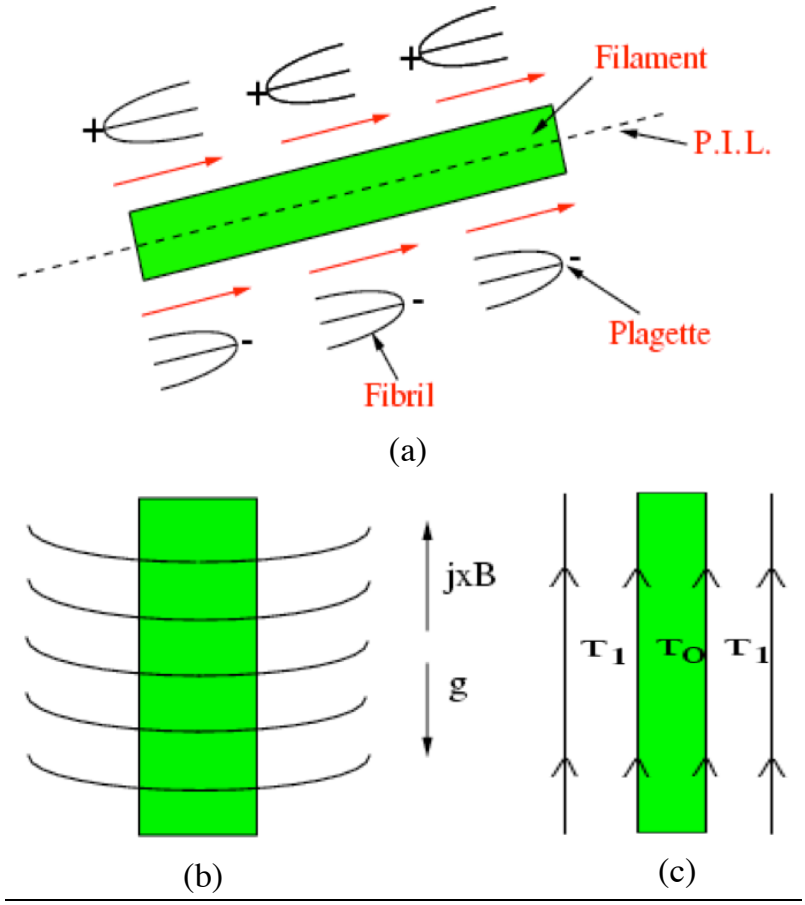


Figure 2: Illustrations of (a) a filament channel, (b) the support of plasma by the magnetic field and (c) the insulation of plasma by a magnetic field.

## 5. Observations of Formation

Current research considers the formation of solar prominences as two distinct problems. The first is the origin of the filament channel and dipped magnetic fields required to support the dense mass against gravity. The second is the origin of the cool dense mass that constitutes the prominence. Both of these topics are discussed in later sections. At the present time, it is unclear how the magnetic field of filament channels and filaments form along the PIL. This represents a key topic for solar physics, since filament channels and filaments represent locations where the build-up and transport of magnetic helicity and energy across the Sun may be studied. Each of these processes are fundamental to the solar cycle and for explaining eruptive phenomena.

Very few examples of the formation of filament channels and filaments have ever been observed. Those observations that do exist may be split into two categories:

(i) filament formation due to surface motions reconfiguring existing coronal magnetic fields (Gaizauskas et al., 1997, 2000; Schmieder et al., 2004; Wang & Muglach, 2007),

(ii) the emergence of horizontal magnetic-flux ropes from the convective zone into the corona (Lites and Low, 1997; Okamoto et al., 2008, 2009).

These two categories can however be reconciled when the filament type and location are considered. In these observations, long-lived Intermediate or Quiescient Filaments are formed as a consequence of the reconfiguration of coronal fields. The observations of Gaizauskas et al. (1997, 2000) show that a key element for the formation of these filaments is the injection of magnetic helicity from activity complexes which is then transported and localised along PILs through the convergence and cancellation of magnetic flux. In contrast, the filaments observed in the second category are unstable active region filaments. Lites and Low (1997) analyse a series of vector magnetic-field measurements and interpret the observations as a horizontal magnetic-flux rope emerging through the photosphere. Present observations suggest that two possible mechanisms of filament formation may exist in different magnetic environments on the Sun. This will be further discussed in the section on Magnetic Field Models.

## 6. Fine-Scale Structure

A wide variety of fine-scale structures may be found for both prominences at the limb and filaments on the disk. When viewed on the solar disk at very high resolution in Hα, the spine and barbs of both intermediate and quiescent filaments are seen to be composed of many thin threads (Lin et al., 2008a, Figure 3a). These thin threads are at the limit of current spatial resolution (100-200km, Lin et al., 2005, 2008a) and are believed to be the basic building blocks of filaments. The thin threads are aligned with the local magnetic field and are believed to outline part of a much longer field line that has a dipped structure, where only the dipped portion is visible (Heinzel and Anzer 2006). While individual filaments may last for many days, each thread has a lifetime of only a few minutes to hours. Thus, while IF and QF are globally very stable structures, their small-scale building blocks are continuously evolving. Observations by Lin et al. (2005) showed that the threads are not static but exhibit sideways motions with a speed around 2-3km/s. In addition to the sideways motions, the threads also display counter-streaming motions. Surrounding each cool thread there are prominence-corona transition regions (PCTRs), one along and the other across the field line where the temperature rises sharply to coronal values. Spectral observations taken by SoHO/SUMER in hydrogen Lyman lines indicate that there are many threads along a given line of sight. Through modelling the fine-scale structure of the threads along with the PCTR both along and across the field lines, Gunar et al. (2008) were able to successfully reproduce the SoHo/SUMER observations when the threads move relative to each other with velocities of +/- 10km/s.

When solar prominences are viewed at high resolution on the limb, a wide variety of structures are found, depending on the type of prominence being observed. Okamoto et al. (2007) found that an active-region prominence is composed of mainly horizontal threads (Figure 3b). In contrast to this, Berger et al. (2008) found that a large hedge-row prominence takes the form of a sheet-like structure with both bright quasi-vertical threads and dark inclusions (Figure 3c). The bright structures corresponded to downflow streams (~10km/s), while the dark inclusions are up-flows (~20km/s). At the present time, the relationship between these quasi-vertical threads and the magnetic field in hedgerow prominences is not well understood. However, using line-of -sight Doppler velocities, Schmieder et al. (2010) showed that in conjunction with the vertical motions there are also horizontal velocities of the same magnitude. This indicated

that there is in fact an inclined structure where the observed vertical motions were a consequence of plane-of-sky projection effects.

One major issue still to be tackled relates the various structures observed in filaments on the disk to those seen in prominences at the limb. In particular, it must be determined if the plasma observed on the solar disk in the form of thin threads has the same structures as observed at the limb as quasi-vertical threads. Only through detailed 3D MHD and radiative-transfer modelling will this be resolved (Heinzel et al. 2015; Gunar & Mackay, 2015a, 2015b, 2016).

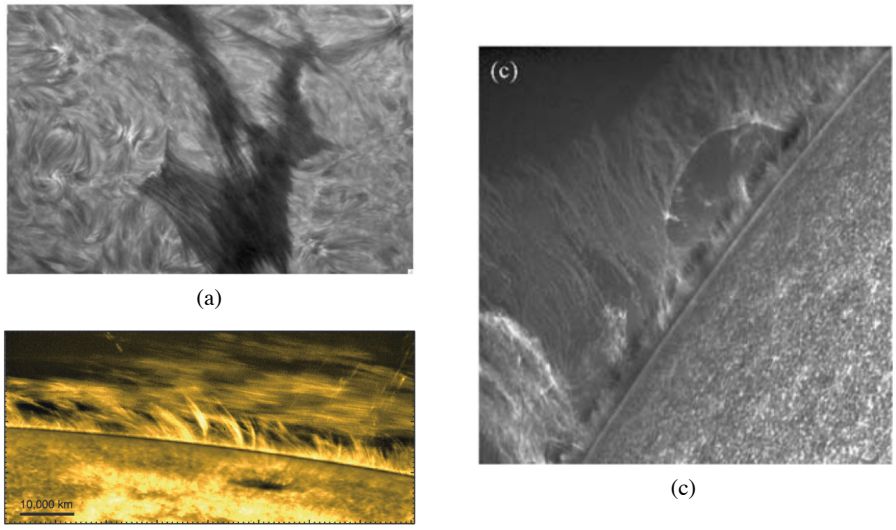


(a) (b) (c)

Figure 3: (a) High resolution Hα image of a filament from the Swedish Solar Telescope (from Lin et al. 2005a). (b) Hinode/SOT Ca II H image of a prominence (from Okamoto et al (2007). (c) Hinode/SOT Ca II H image of a Hedgerow prominence (courtesy of Tom Berger)

## 7. Global Chirality Patterns

The magnetic field of solar filaments may be categorised into one of two types of chirality, "dextral" or "sinistral". This chirality defines the orientation of the dominant axial magnetic field as viewed by an observer standing on the positive polarity side of the filament channel (Martin et al., 1992). In a dextral filament, the axial magnetic field is directed to the right, while for a sinistral filament, it is directed to the left. In theoretical models the chirality of a filament is closely related to the dominant magnetic helicity within the filament, where dextral filaments have negative helicity and sinistral filaments positive helicity (Aulanier et al., 1998; Mackay et al., 1999;). To determine the chirality of solar filaments, a number of techniques may be applied. These techniques include:

(i) the orientation of chromospheric fibrils in high resolution Hα images (Martin et al., 1994),
(ii) the one-to-one relationship between filament chirality and their barbs (dextral/sinistral filaments have right/left bearing barbs, Pevtsov et al., 2003),
(iii) direct magnetic-field measurements (Rust, 1967; Leroy, 1989) and finally
(iv) coronal cells observed at 193 Å (Sheeley et al., 2013).

To date, the most common method used to determine chirality has been filament barbs where automated techniques have been developed (Bernasconi et al., 2005). All of the above techniques, except for the direct magnetic-field measurements, use indirect relationships

between the filaments axial magnetic field and structural elements of the filament channel or filament. At the present time, no studies have compared results of filament chirality determined from both direct and indirect techniques.

One of the most important aspects of filament chirality is that it exhibits a global hemispheric pattern where "dextral" filaments dominate in the Northern Hemisphere and "sinistral" filaments in the Southern Hemisphere (Martin et al., 1994; Pevtsov et al., 2003). This chirality pattern describes a global pattern of magnetic helicity that exists on the Sun and therefore outlines underlying physical processes for the production and evolution of non-potential solar magnetic fields. The global pattern is not an absolute rule, but rather a percentage rule, where the relationship of dominant to minority chirality in each hemisphere is approximately 75:25%. Observations have also shown that the chirality pattern strengthens with increasing latitude and is strongest for quiescent and intermediate filaments.

A number of theoretical attempts have aimed at explaining the hemispheric pattern of filaments through considering the underlying physical processes for the generation and evolution of non-potential magnetic fields on the Sun. Yeates et al. (2008) carried out a detailed one-to-one comparison of observed filament chirality with that produced through a global non-potential evolution model (Mackay & van Ballegooijen, 2006). The global non-potential model included the effects of differential rotation, meridional flow and surface diffusion, along with the emergence of new magnetic bipoles containing either positive or negative helicity (Mackay & van Ballegooijen, 2005). By emerging dominantly negative helicity bipoles in the northern hemisphere and positive in the south, the authors followed the transport and dispersal of magnetic helicity and magnetic flux out from active regions. They were able to obtain a 95% agreement with observations for low- to mid-latitude filaments. Further studies extending over a solar cycle (Yeates & Mackay, 2012) showed that an excellent agreement could be obtained at all latitudes in the rising phase of the cycle, while in the declining phase, minority chirality dominated at mid- to high-latitudes in disagreement with the observations. While the mechanisms used by Yeates et al. (2008) were mainly large-scale mechanisms, Antiochos (2013) put forward an alternative model called the helicity condensation model. In this model, small-scale vortical motions in granules or super-granules inject helicity continuously across the entire solar surface. The model assumes that within the northern/southern hemispheres, a positive/negative vorticity is present within these convective cells, where this vorticity injects negative/positive helicity. Assuming that this sign of vorticity occurs over large length scales and in a coherent pattern in each hemisphere, the helicity may be redistributed to lie along PILs through the process of magnetic reconnection. Using a macroscopic model, Mackay, DeVore and Antiochos (2014) and Mackay et al. (2018) determined that the minimum value of vorticity required to reproduce the hemispheric pattern of filaments is around $5 \times 10^{-6} s^{-1}$. To date, observations have still to determine if such values of vorticity exist within convective cells, along with coherence and latitudinal distribution.

## 8. Origin of Mass

It is generally recognised that the mass in solar prominences must originate from chromospheric heights, as there is insufficient mass in the corona to explain a large quiescent filament (Pikel'ner, 1971; Saito & Tandberg-Hanssen, 1973; Zirker et al., 1994). It is still unclear how the mass is transported to the corona and into the dipped field lines. Studying the origin of the mass within prominences is therefore a key area of research.

A number of mechanisms to transport mass into the corona have been put forward. Two distinct physical processes are considered. The first is due to magnetic forces which either lift

(Levitation models) or inject (Injection models) the cool plasma from chromospheric heights into the corona. The second possibility uses localised chromospheric heating and thermal pressure forces to evaporate mass into the corona which then subsequently condenses (Thermal non-equilibrium model). All of these mechanisms have some observational basis. However, to explain the formation of prominences, a mechanism must satisfy a number of observational constraints, as discussed in Karpen (2015).

The basic concept behind injection is that cool chromospheric material is injected into the corona with sufficient speed that the material reaches the high dipped coronal field lines of the filament channel. This mechanism is most likely relevant in low-lying active-region filaments (Chae, 2003). This model is motivated by observations of flux cancellation (Martin, 1998; Wang & Muglach 2007) occurring below filaments, where magnetic reconnection injects the mass into the corona (Wang, 1998; Chae, 2001). While the basic physical process is well understood, a major issue is that the magnetic reconnection needs to be at chromospheric heights, which may not always be the case. While relevant for active region filaments, it is unlikely to explain the mass found in quiescent filaments, as the material would have to be injected to a height of approximately 50Mm.

The basic principle behind levitation models is that cool chromospheric plasma is lifted to coronal heights by rising magnetic field lines, where the field lines move perpendicular to the direction of the field. Two distinct forms of this process have been considered. In the first, initially unconnected magnetic polarities converge towards one another and flux cancellation and magnetic reconnection takes place (Galsgaard & Longbottom, 1999, von Rekowski & Hood 2008). Alternatively, there may be a horizontal magnetic flux rope lying in the transition region which emerges into the corona. As it emerges, cool material located in the dips is dragged upwards (Rust & Kumar 1994). A major problem with this second scenario is that the axis of the flux rope must rise into the corona, which is not supported by flux emergence simulations (Manchester et al., 2004; Magara, 2006; Archontis & Torok, 2008).

In contrast to the two mechanisms described above, which rely mainly on magnetic forces, the third mechanism, called the "thermal non-equilibrium" model (Antiochos et al., 1999, 2000) uses thermal pressure forces. The basic principle is that when highly localized heating is applied near the chromospheric foot points of magnetic field lines, hot material is evaporated along the field line into the corona. This causes an increase in density along the magnetic field line and subsequently the radiative losses increase. If the heating length scale near the chromosphere is very small compared to the overall length of the field line, thermal conduction along the field line cannot counter the increased radiative losses. Near the middle of the loop a radiatively driven thermal collapse occurs, where the plasma drops to chromospheric temperatures to regain thermal equilibrium (Serio, 1981; Mok, 1990; Antiochos & Klinchuk, 1991). Numerical simulations by Karpen et al. (2001, 2005, 2006) have shown that this technique can explain many observed features of filaments such as stationary or highly dynamic threads and the cyclic process of condensation formation. To date, this model is the most extensively developed and is the leading candidate to explain the origin of mass within quiescent and intermediate filaments. The main outstanding question still to be resolved is the origin of the short-length-scale heating that is required near the chromospheric foot points of the field lines. Whilst it is the leading candidate for Intermediate and Quiescent filaments, the model cannot explain the mass observed within active region prominences, which are too short to allow the radiative collapse to occur. Conversely, one of the previous mechanisms based on magnetic forces is most likely to explain these prominences.

## 9. Oscillations

Quiescent prominences and filaments are known to support a wide variety of large- and small-scale oscillations. The first detected oscillation was by Ramsey and Smith (1966), when a solar flare induced a large-amplitude (~20km/s) oscillation. Small-amplitude oscillations have been detected from both ground (Tsubaki, 1988; Oliver 1999; Oliver & Ballester 2002) and space (Ning et al., 2009; Blanco et al., 1999; Foullon et al., 2004). The key characteristics of these oscillations are:

(i) they have an amplitude of (~1-3km/s),
(ii) they can be categorised into three separate period ranges (Short P<10 min, Intermediate 10<P<40min, long P>40min),
(iii) they are local in nature, but can occur in coherent patterns over large spatial ranges.
(iv) both oscillations and flows occur together,
(v) the oscillations are strongly damped in time within 1-3 periods (Oliver & Ballester 2002).

The importance of small-amplitude oscillations is that they may be used to carry out seismology of the local coronal environment to infer the physical properties and internal structure of prominences (Ballester, 2006, 2014). This provides an indirect measurement of properties such as Alfven speed, magnetic-field strength and the shear angle of the field. At the present time, the origin of these small-scale amplitude oscillations is unknown. A review of current understanding of damping mechanisms can be found in Solar et al., (2014).

## 10. Eruptions

Whilst solar filaments and prominences are stable structures, eruptions of these phenomena can occur. The eruptions can result in material being ejected from the solar corona into interplanetary space, where it may lead to a coronal mass ejection (CME). CMEs can directly impact the Earth and lead to space-weather events. Whilst this is one way in which a filament may end its life, it is also possible for the material to disappear in-situ or drain back down to the chromosphere.

Observations show that filament eruptions take the form of a two-stage process. In the first stage there is a slow rise phase (0.1-1km/s) that may last for several hours before the onset of the full eruption. During this stage, both active region and quiescent prominences exhibit enhanced non-thermal motions where on the solar disk the filament becomes darker, while at the limb it becomes brighter. The second stage involves the rapid outward expansion of the filament material, where a wide range of velocities are possible (100-1000km/s). During some eruptions, not all of the prominence material is ejected into interplanetary space and parts may fall back into the Sun as a failed eruption (Wang & Sheeley, 2002). It is also possible for a partial eruption to occur, where part of the filament remains in a stable configuration in the filament channel. Even when an eruption occurs and the filament material is ejected, often the underlying magnetic field configuration of the filament channel remains and a filament or prominence can be seen to reform within a few hours to days.

Many different mechanisms have been proposed to explain the onset of prominence eruptions and subsequent CMEs. These mechanisms include: flux cancellation followed by loss of equilibrium, triggering by flux emergence, tether cutting, triggering by flares and finally magnetic breakout. For detailed reviews of all of these mechanisms see Aulanier (2014), van Driel-Gesztelyi and Culhane (2009) and Parenti (2014a).

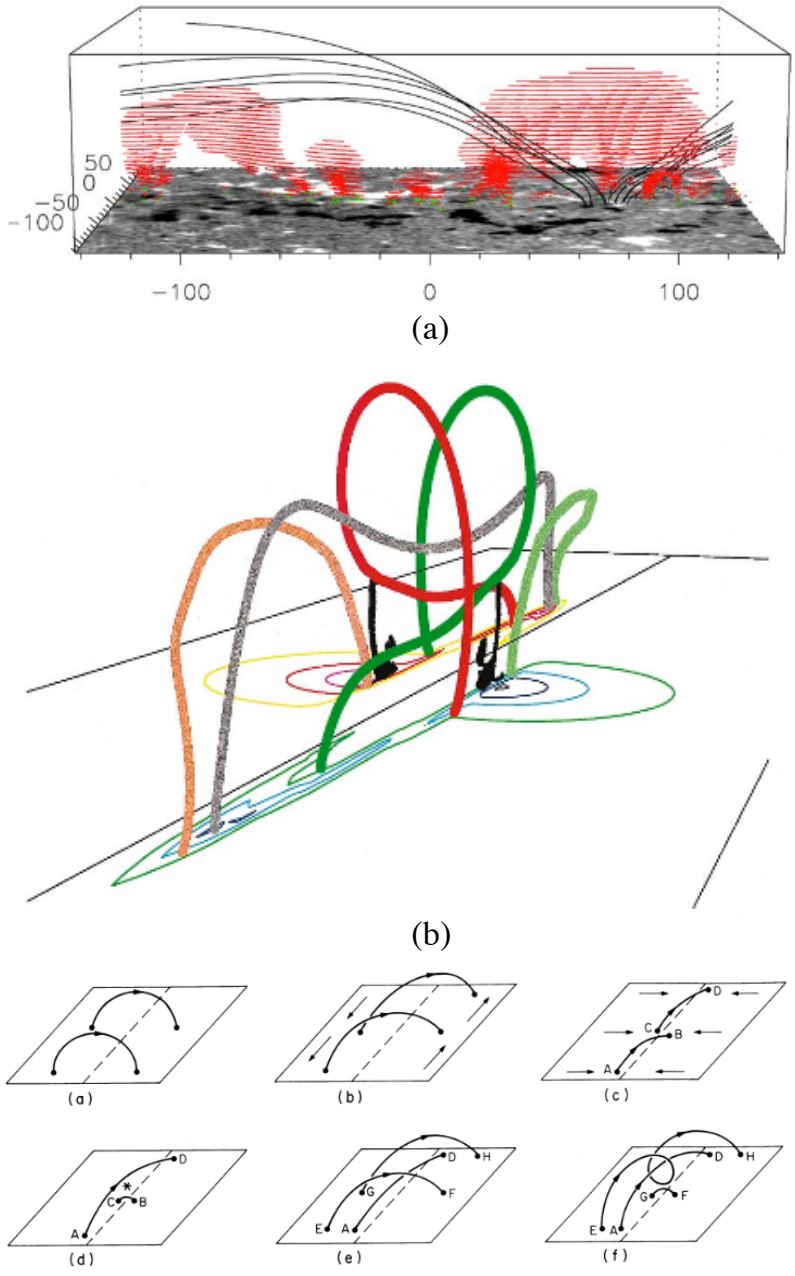


*Figure* 4 *: Illustration of magnetic-field models: (a) The force-free flux-rope model of Dudik et al. 2008. (b) The sheared arcade model of DeVore and Antiochos 2000. (c) The shearing and flux cancellation model of van Ballegooijen and Martens (1989).*

## 11. Magnetic Field Models

Observations of filaments and filament channels clearly show that they are embedded in highly non-potential magnetic fields, where the dominant component of the field lies along the PIL and filament axis. These axial fields are described as being strongly sheared. Since magnetic fields can only be routinely measured at photospheric heights, the nature of magnetic fields

and associated electric-current systems within filaments and filament channels are not well understood. Mackay et al. (2020) carried out a comparison of direct magnetic-field measurements made within a prominence with the results of a theoretical magnetic-field model. Much of the understanding of prominence magnetic fields comes from theoretical modelling, where a vast range of models using a variety of approximations has been produced. These models may be split into two distinct types. The first are static models which consider the magnetic field at a single instant in time. The second are dynamic models which aim to explain how the magnetic field evolves into its strongly sheared state.

## 11.1 Static Models

Two categories of static models exist within the literature. In the first type the weight of the prominence plasma plays a key role in creating the dips in the field lines. The first model to consider this was put forward by Kippenhahn and Schluter (1957). Since then a wide range of extensions of this model have been developed (Malherbe & Priest 1983; Hood & Anzer, 1990; Heinzel & Anzer, 2001; Low & Petrie, 2005). In contrast, the second type assumes that even without the presence of the prominence mass, the magnetic field is naturally dipped. In this approximation it is assumed that the plasma beta is low ($\beta << 1$) such that the plasma does not play a central role or significantly perturb the dip. Often these models use the force-free approximation and may themselves be sub-divided into two categories: flux rope and sheared arcade models.

In some static models, the magnetic field of the filament is assumed to be a horizontally lying force-free flux rope (Kupperus & Raadu, 1974,; van Ballegooijen & Martens, 1989; Rust & Kumar, 1994, Aulanier & Demoulin, 1998; Gibson & Fan, 2006) where the mass of the filament is located in helical dips. Both strongly and weakly twisted flux ropes have been considered. However, only the weakly twisted flux ropes are consistent with direct magnetic-field measurements and the observed axial flows in non-erupting prominences. One key feature of these models is that there are two distinct and independent flux systems, namely, the magnetic field of the flux rope and the overlying arcade that is required to maintain the flux rope in a stable configuration. Flux-rope models naturally contain the mass of the filament in inverse polarity magnetic fields and thus are consistent with direct magnetic-field measurements. The basic force-free flux-rope models have been extended to consider Linear-MHS (Aulanier & Demoulin, 2003; Dukik et al., 2008) and NLFFF (van Ballegooijen, 2004; Mackay and van Ballegooijen, 2009) models along with the direct extrapolation of these fields from magnetograms. These models have been extremely successful in reproducing individual features of observed filaments, such as filament barbs and breaks in the body of filaments (Figure 4a). An alternative model to the flux-rope model is the sheared arcade model (Antiochos et al., 1994; DeVore and Antiochos, 2000) ,where there is only a single flux system. The model of DeVore and Antiochos (2000) shows that in sheared arcades both regions of normal and inverse polarity may exist (Figure 4b).

## 11.2 Dynamic Models

A wide range of theoretical models have been developed to explain how filament channels with a dipped magnetic field can be produced. Due to the lack of observations of the formation of filaments and filament channels, a number of physical mechanisms have been used. In line with the observations of filament formation these models may be split into two categories: surface and sub-surface models. A full discussion of these models and the variety of mechanisms that they employ can be found in Mackay (2015), where a few selected cases are now discussed.

One of the first surface models where surface motions are applied to reconfigure a pre-existing coronal field was developed by van Ballegooijen and Martens (1989) and is illustrated in Figure 4c. To produce the filament channel, a number of mechanisms are used and they occur in a specific order. First, shearing motions act on a coronal arcade, which plays the dual role of separating the foot points and creating an axial field along the PIL (see Figs. 4c panel (a) and (b)). The axial field is then enhanced and localized along the PIL by convergence or diffusion of the magnetic field towards the PIL. This convergence brings foot points together where reconnection produces a long axial field line along the PIL (Figs. 4c panel (c) and (d)). Through further repetitions of this process, dipped magnetic field lines are produced (Figs. 4c panel (e) and (f)). While van Ballegooijen and Martens (1989) developed a conceptual model, Mackay et al. (2000) and Mackay and van Ballegooijen (2001) carried out 3D numerical simulations of this process. In contrast, DeVore and Antiochos (2000) considered how a filament channel could be produced in a single bipolar configuration when it is subjected to a strong shearing motion along the PIL. The authors found that once the foot points of the field lines were sheared a distance comparable to the bipole width, a dipped magnetic field configuration forms.

For models which rely on sub-surface mechanisms, the key features are described in the papers by Low (1994) and Rust and Kumar (1994). In these papers the filament formation is the result of a horizontal twisted magnetic flux tube that emerges through the photosphere and rises into the corona. As it rises, it drags cool dense material with it, to produce the mass of the prominence. The feasibility of this process has however been questioned by flux emergence simulations, which show that, when invoking buoyancy and magnetic buoyancy instabilities, the axis of the flux rope does not rise through the photosphere (Moreno-Insertis, 2004; Archontis et al., 2004). However, the process of flux emergence can still explain small active region filaments, as it can produce a coronal flux rope with dips through a secondary magnetic reconnection process (Manchester et al., 2004; Archontis and Török, 2008).

## 12. Conclusions

Research into solar prominences spans many distinct areas from observational studies to theoretical models and numerical simulations. Each of these areas has been applied to the many diverse phenomena that arise in prominences, ranging from those found at the smallest observable spatial scales to the large-scale global patterns. The combination of theoretical and observational studies has led to a good understanding of solar prominences. While this is the case there are still many unanswered questions. Some of these questions include, but are not restricted to:

1. What physical processes produce the thin horizontal threads and why do gaps between these threads occur? Why do some structures exhibit horizontal motions while other exhibit both vertical structure and motions?

2. What is the orientation of the magnetic field in barbs and how/why do barbs form?

3. What is the formation mechanism of filament channels and do different mechanisms act at different locations on the Sun? Why do filament channels and filaments form at some locations along a PIL and not others?

4. Is the basic magnetic field configuration of a filament a sheared arcade or twisted magnetic-flux rope? Or do both arise under specific circumstances?

5. What thermodynamic processes explain the origin of the cool dense material along with the observed flows and oscillations?

6. How is the hemispheric pattern of filaments related to the 3D dynamo and evolution of helicity across the Sun?

7. Why does the eruption of some prominences lead to material being ejected from the Sun in the form of a CME, while other prominences erupt but fall back into the Sun?

Answers to these questions can only be found with coordinated observations from both ground and space, spanning a wide range of wavelengths, combined with state-of-the-art data-driven theoretical models. With this coordinated approach, the true origin and nature of solar prominences may be unraveled.

**References**

Alexander, C.E., Walsh, RW., Regnier, S., et al. (2013). Anti-parallel EUV Flows Observed along Active Region Filament Threads with Hi-C. Astrophysical Journal Letters, 775, L32.

Antiochos, S.K., & Klimchuk, J.A. (1991). A model for the formation of solar prominences. Astrophysical Journal, 378, 372.

Antiochos, S.K., Dahlburg, R.B., & Klimchuk, J.A. (1994). The magnetic field of solar prominences. Astrophysical Journal Letters, 420, L41.

Antiochos, S.K., MacNeice, P.J., Spicer, D.S., & Klimchuk, J.A. (1999). The Dynamic Formation of Prominence Condensations. Astrophysical Journal, 512, 985.

Antiochos, S.K., MacNeice, P.J., & Spicer, D.S. (2000). The Thermal Nonequilibrium of Prominences. Astrophysical Journal, 536, 494.

Antiochos, S.K. (2013). Helicity Condensation as the Origin of Coronal and Solar Wind Structure. Astrophysical Journal, 772, 72.

Archontis, V., & Torok, T. (2008). Eruption of magnetic flux ropes during flux emergence. Astronomy and Astrophysics, 492, L35.

Aulanier, G., & Demoulin, P. (1998). 3-D magnetic configurations supporting prominences. I. The natural presence of lateral feet. Astronomy and Astrophysics, 329, 1125.

Aulanier, G., & Demoulin, P. (2003). Amplitude and orientation of prominence magnetic fields from constant-alpha magnetohydrostatic models. Astronomy and Astrophysics, 402, 769.

Aulanier, G. (2014). The physical mechanisms that initiate and drive solar eruptions. Nature of Prominences and their Role in Space Weather, 300, 184.

Babcock, H. D., & Babcock, H. W. (1955). The sun's magnetic field, 1952–1954. The Astrophysical Journal, 121, 3.

Ballester, J.L. (2006), Seismology of Prominence-Fine structures: Observations and Theory. Space Science Reviews, 122, 129.

Ballester, J.L. (2014). Prominence Seismology. Nature of Prominences and their Role in Space Weather, 300, 30.

Bernasconi, P.N., Rust, D.M., & Hakim, D. (2005). Advanced Automated Solar Filament Detection and Characterization Code: Description, Performance, And Results. Solar Physics, 228, 97.

Blanco, S., Bocchialini, K., Costa, A., et al. (1999). Multiresolution wavelet analysis of SUMER/SOHO observations in a solar prominence. Solar Physics, 186, 281.

Berger, T.E., Shine, R.A., Slater, G.L., et al. (2008). Hinode SOT Observations of Solar Quiescent Prominence Dynamics. Astrophysical Journal Letters, 676, L89.

Berger, T.E., Liu, W., & Low, B.C. (2012). SDO/AIA Detection of Solar Prominence Formation within a Coronal Cavity. Astrophysical Journal Letters, 758, L37.

Bommier, V., & Leroy, J.L. (1998). Global Pattern of the Magnetic Field Vectors Above Neutral Lines from 1974 to 1982: Pic-du-Midi Observations of Prominences. IAU Colloq. 167: New Perspectives on Solar Prominences, 150, 434.

Casini, R., Lopez Ariste, A., Tomczyk, S., & Lites, B.W. (2003). Magnetic Maps of Prominences from Full Stokes Analysis of the He I D3 Line. Astrophysical Journal Letters, 598, L67.

Chae, J. (2001). Observational Determination of the Rate of Magnetic Helicity Transport through the Solar Surface via the Horizontal Motion of Field Line Foot Points. Astrophysical Journal Letters, 560, L95.

Chae, J. (2003). The Formation of a Prominence in NOAA Active Region 8668. II. Trace Observations of Jets and Eruptions Associated with Cancelling Magnetic Features. Astrophysical Journal, 584, 1084.

D'Azambuja, L., & D'Azambuja, M. (1948). Etude d'ensemble des protubérances solaires et deleur évolution, Annales de l'Observatoire de Paris, Tome VI, Gauthiers-Villars.

Dunn, R. (1960). Photometry of the solar chromosphere, Ph.D. Thesis, Harvard University.

DeVore, C.R., & Antiochos, S.K. (2000). Dynamical Formation and Stability of Helical Prominence Magnetic Fields. Astrophysical Journal, 539, 954.

Dudik, J., Aulanier, G., Schmieder, B., Bommier, V., & Roudier, T. (2008). Topological Departures from Translational Invariance along a Filament Observed by THEMIS. Solar Physics, 248, 29.

Dunn, R. (1965). Sacramento Peak Obs. Contr. Report #87, Fig. 36, p. 80.

Engvold, O. (2015). Description and Classification of Prominences. Solar Prominences, 415, 31.

Foukal, P. (1971). Morphological Relationships in the Chromospheric Hα Fine Structure. Solar Physics, 19, 59.

Foukal, P. (1971). Hα Fine Structure and the Chromospheric Field, Solar Physics, 20, 298.

Foullon, C., Verwichte, E., & Nakariakov, V.M. (2004). Detection of ultra-long-period oscillations in an EUV filament. Astronomy and Astrophysics, 427, L5.

Fuller, J., Gibson, SE., de Toma, G., & Fan, Y. (2008). Observing the Unobservable? Modeling Coronal Cavity Densities. Astrophysical Journal, 678, 515.

Gaizauskas, V. (1998). Filament Channels: Essential Ingredients for Filament Formation. IAU Colloq.~167: New Perspectives on Solar Prominences, 150, 257.

Galsgaard, K., & Longbottom, A.W. (1999). Formation of Solar Prominences by Flux Convergence. Astrophysical Journal, 510, 444.

Gibson, S.E., & Fan, Y. (2006). Coronal prominence structure and dynamics: A magnetic flux rope interpretation. Journal of Geophysical Research (Space Physics), 111, A12103.

Gibson, S.E., Kucera, T.A., Rastawicki, D., et al. (2010). Three-dimensional Morphology of a Coronal Prominence Cavity. Astrophysical Journal, 724, 1133.

Gibson, S. (2014). Magnetism and the Invisible Man: The mysteries of coronal cavities. Nature of Prominences and their Role in Space Weather, 300, 139.

Gunar, S., Heinzel, P., Anzer, U., & Schmieder, B. (2008). On Lyman-line asymmetries in quiescent prominences. Astronomy and Astrophysics, 490, 307.

Gunar, S., & Mackay, D.H. (2015a). 3D Whole-Prominence Fine Structure Modeling. Astrophysical Journal, 803, 64.

Gunar, S., & Mackay, D.H. (2015b). 3D Whole-prominence Fine Structure Modeling. II. Prominence Evolution. Astrophysical Journal, 812, 93.

Gunar, S., & Mackay, D.H. (2016). Properties of the prominence magnetic field and plasma distributions as obtained from 3D whole-prominence fine structure modelling. Astronomy and Astrophysics, 592, A60.

Heinzel, P., & Anzer, U. (2001). Prominence fine structures in a magnetic equilibrium: Two-dimensional models with multilevel radiative transfer. Astronomy and Astrophysics, 375, 1082.

Heinzel, P., & Anzer, U. (2006). On the Fine Structure of Solar Prominences. Astrophysical Journal, 643, 65.

Heinzel, P. (2015). Radiative Transfer in Solar Prominences. Solar Prominences, 415, 103.

Heinzel, P., Gunár, S & Anzer, U. (2015). Fast approximate radiative transfer method for visualizing the fine structure of prominences in the hydrogen Hα line. Astronomy and Astrophysics, 579, 16.

Hood, A.W., & Anzer, U. (1990). A model for quiescent solar prominences with normal polarity. Solar Physics, 126, 117.

Hyder, C.L. (1965). The Polarization of Emission Lines in Astronomy. II. Prominence Emission-Line Polarization and Prominence Magnetic Fields. Astrophysical Journal, 141, 1374.

Karpen, J.T., Antiochos, S.K., Hohensee, M., Klimchuk, J.A., & MacNeice, P.J. (2001). Are Magnetic Dips Necessary for Prominence Formation?. Astrophysical Journal Letters, 553, L85.

Karpen, J.T., Tanner, S.E.M., Antiochos, S.K., & DeVore, C.R. (2005). Prominence Formation by Thermal Nonequilibrium in the Sheared-Arcade Model. Astrophysical Journal, 635, 1319.

Karpen, J.T., Antiochos, S.K., & Klimchuk, J.A. (2006). The Origin of High-Speed Motions and Threads in Prominences. Astrophysical Journal, 637, 531.

Karpen, J.T. (2015), Solar Prominences, 415, 237.

Kippenhahn, R., & Schlüter, A. (1957). Eine Theorie der solaren Filamente. Mit 7 Textabbildungen. Zeitschrift fur Astrophysik, 43, 3.

Kuperus, M., & Raadu, M. A. (1974). The support of prominences formed in neutral sheets, Astronomy and Astrophysics, 31, 189.

Leroy, J.-L., Ratier, G., & Bommier, V. (1977). The polarization of the D3 emission line in Prominences, Astronomy and Astrophysics, 54, 811.

Leroy, J.L., Bommier, V., & Sahal-Brechot, S. (1983). The magnetic field in the prominences of the polar crown. Solar Physics, 83, 135.

Leroy, J.L. (1989). Observation of prominence magnetic fields. Dynamics and Structure of Quiescent Solar Prominences, 150, 77.

Lin, Y., Engvold, O.R., & Wiik, J.E. 2003. Counterstreaming in a Large Polar Crown Filament. Solar Physics, 216, 109.

Lin, Y., Martin, S.F., & Engvold, O. (2008a). Filament Substructures and their Interrelation. Subsurface and Atmospheric Influences on Solar Activity, 383, 235.

Lin, Y., Engvold, O., Rouppe van der Voort, L., Wiik, J.E., & Berger, T.E. (2005a). Thin Threads of Solar Filaments. Solar Physics, 226, 239.

Lites, B.W. (2005). Magnetic Flux Ropes in the Solar Photosphere: The Vector Magnetic Field under Active Region Filaments. Astrophysical Journal, 622, 1275.

López Ariste, A., Aulanier, G., Schmieder, B., & Sainz Dalda (2006). A First observation of bald patches in a filament channel and at a barb endpoint, Astronomy and Astrophysics, 456, 725.

López Ariste, A., & Aulanier, G. (2007). Unveiling the Magnetic Field Topology of Prominences. The Physics of Chromospheric Plasmas, 368.

López Ariste, A. (2015). Magnetometry of Prominences. Solar Prominences, 415, 179.

Low, B.C. ,& Hundhausen, J.R. (1995). Magnetostatic structures of the solar corona. 2: The magnetic topology of quiescent prominences. Astrophysical Journal, 443, 818.

Low, B.C., & Petrie, G.J.D. (2005). The Internal Structures and Dynamics of Solar Quiescent Prominences. Astrophysical Journal, 626, 551.

Ning, Z., Cao, W., Okamoto, T.J., Ichimoto, K., & Qu, Z.Q. (2009). Small-scale oscillations in a quiescent prominence observed by HINODE/SOT. Astronomy and Astrophysics, 499, 595.

Mackay, D.H., Longbottom, A.W., & Priest, E.R. (1999). Dipped Magnetic Field Configurations Associated with Filaments and Barbs. Solar Physics, 185, 87.

Mackay, D.H., & van Ballegooijen, A.A. (2005). New Results in Modeling the Hemispheric Pattern of Solar Filaments. Astrophysical Journal Letters, 621, L77.

Mackay, D.H., & van Ballegooijen, A.A. (2006). Models of the Large-Scale Corona. I. Formation, Evolution, and Liftoff of Magnetic Flux Ropes. Astrophysical Journal, 641, 577.

Mackay, D.H., Gaizauskas, V., & Yeates, A.R. (2008). Where Do Solar Filaments Form?: Consequences for Theoretical Models. Solar Physics, 248, 51.

Mackay, D.H., & van Ballegooijen, A.A., A Non-Linear Force-Free Field Model for the Evolving Magnetic Structure of Solar Filaments, (2009), Solar Physics, 260, 321.

Mackay, D.H., DeVore, C.R., & Antiochos, S.K. (2014). Global-scale Consequences of Magnetic-helicity Injection and Condensation on the Sun. Astrophysical Journal, 784, 164.

Mackay, D.H., DeVore, C.R., Antiochos, S.K., & Yeates, A.R. (2018). Magnetic Helicity Condensation and the Solar Cycle. Astrophysical Journal, 869, 62.

Mackay, D.H, Schmieder, B., López Ariste, A. & Su, Y. (2020). Modelling and Observations: Comparison of the magnetic field properties in a prominence, Astronomy and Astrophysics, 637, 3.

Magara, T. (2006). Dynamic and Topological Features of Photospheric and Coronal Activities Produced by Flux Emergence in the Sun, Astrophysical Journal, 653, 1499.

Malherbe, J.M., & Priest, E.R., (1983). Current sheet models for solar prominences. I Magnetohydrostatics of support and evolution through quasi-static models. Astronomy and Astrophysics, 123, 80.

Manchester, W., IV, Gombosi, T., DeZeeuw, D., & Fan, Y. (2004). Eruption of a Buoyantly Emerging Magnetic Flux Rope. Astrophysical Journal, 610, 588.

Martin, S.F., Marquette, W.H., & Bilimoria, R. (1992). The Solar Cycle Pattern in the Direction of the Magnetic Field along the Long Axes of Polar Filaments. The Solar Cycle, 27, 53.

Martin, S.F., Bilimoria, R., & Tracadas, P.W. (1994). Magnetic field configurations basic to filament channels and filaments. NATO Advanced Science Institutes (ASI) Series C, 433, 303.

Martin, S.F., & Echols, C.R (1994). An observational and conceptual model of the magnetic field of a filament. NATO Advanced Science Institutes (ASI) Series C, 433, 339.

Martin, S.F (1998). Conditions for the Formation and Maintenance of Filaments. Solar Physics, 182, 107.

Martres, M.J., Michard, R., & Soru-Iscovici, I, (1966). Etude morphologique de la structure magnetique des regions actives en relation avec les phenomenes chromospheriques et les eruptions solaires. II. Localisation des plages brillantes, filaments et eruptions. Annales d'Astrophysique, 29, 249.

Mok, Y., Drake, JF., Schnack, D.D., & van Hoven, G. ,(1990). Prominence formation in a coronal loop. Astrophysical Journal, 359, 228.

Okamoto, T.J., Tsuneta, S., Berger, T.E., et al. (2007). Coronal Transverse Magnetohydrodynamic Waves in a Solar Prominence. Science, 318, 1577.

Okamoto, T.J., Tsuneta, S., Lites, B.W., et al. (2008). Emergence of a Helical Flux Rope under an Active Region Prominence. Astrophysical Journal Letters, 673, L215.

Oliver, R. (1999). Prominence Oscillations: Observations and Theory. Magnetic Fields and Solar Processes, 448, 425.

Oliver, R., & Ballester, J.L (2002), Oscillations in Quiescent Solar Prominences Observations and Theory. Solar Physics, 206, 45.

Paletou, F., & Aulanier, G. (2003). Spectropolarimetry of Solar Prominences. Solar Polarization, 307, 458.

Paletou, F. (2008). The magnetic field of solar prominences. SF2A-2008, 559.

Parenti, S. (2014). Solar Prominences: Observations. Living Reviews in Solar Physics, 11, 1.

Pecseli, H., & Engvold, O. (2000). Modeling of prominence threads in magnetic fields: Levitation by incompressible MHD waves. Solar Physics, 194, 73.

Pikel'er, S.B. (1971). Origin of Quiescent Prominences. Solar Physics, 17, 44.

Pevtsov, A.A., Balasubramaniam, K.S., & Rogers, J.W. (2003). Chirality of Chromospheric Filaments. Astrophysical Journal, 595, 500.

Ramsey, H.E., & Smith, S.F. (1966). Flare-initiated filament oscillations. Astrophysical Journal, 71, 197.

Rust, D.M. (1967). Magnetic Fields in Quiescent Solar Prominences. I. Observations. Astrophysical Journal, 150, 313.

Rust, D.M., & Kumar, A. (1994). Helical magnetic fields in filaments. Solar Physics, 155, 69.

Sahal-Bréchot, S., Bommier, V., & Leroy, J.-L. (1977). The Hanle effect and the determination of magnetic fields in solar prominences. Astronomy and Astrophysics, 59, 223.

Saito, K. &Tandberg-Hanssen, E. (1973). The Arch Systems, Cavities, and Prominences in the Helmet Streamer Observed at the Solar Eclipse, November 12, 1966. Solar Physics, 31, 105.

Schmieder, B., Chandra, R., Berlicki, A. & Mein, P. (2010). Velocity vectors of a quiescent prominence observed by Hinode/SOT and the MSDP (Meudon), Astronomy and Astrophysics, 514, A68.

Serio, S., Peres, G., Vaiana, G.S., Golub, L., & Rosner, R. (1981). Closed coronal structures. II - Generalized hydrostatic model. Astrophysical Journal, 243, 288.

Sheeley, N.R., Jr., Martin, S.F., Panasenco, O., & Warren, H.P. (2013). Using Coronal Cells to Infer the Magnetic Field Structure and Chirality of Filament Channels. Astrophysical Journal, 772, 88.

Soler, R., Oliver, R., & Ballester, J.L. (2014). The damping of transverse oscillations of prominence threads: a comparative study. Nature of Prominences and their Role in Space Weather, 300, 48.

Tandberg-Hanssen, E. (1995). The nature of solar prominences. Astrophysics and Space Science Library, 199.

Tang, F, (1987) Quiescent prominences - Where are they formed? Solar Physics, 107, 233.

Tsubaki, T., Toyoda, M., Suematsu, Y., & Gamboa, G.A.R. (1988). New evidence for oscillatory motions in a quiescent prominence. Publications of the Astronomical Society of Japan, 40, 121.

van Ballegooijen, A.A., & Martens, P.C.H. (1989). Formation and eruption of solar prominences. Astrophysical Journal, 343, 971.

van Ballegooijen, A.A. (2004). Observations and Modeling of a Filament on the Sun. Astrophysical Journal, 612, 519.

van Driel-Gesztelyi, L., & Culhane, J.~L. (2009). The Origin and Dynamics of Solar Magnetism. Space Sciences Series of ISSI, Volume 32, Springer New York, p.351.

Vassenius, B. (1733). Observation de l'éclipse totale de Soleil avec demeure, faite à Gothebourg en Suède à 57ı 40' 54 le 2 Mai 1733, Philosophical Transactions of the Royal Society of London, 3.

von Rekowski, B., & Hood, A.W. (2008). Photospheric cancelling magnetic features and associated phenomena in a stratified solar atmosphere. Monthly Notices of the Royal Astronomical Society, 385, 1792.

Wang, Y.-M. (1999). The Jet like Nature of He II λ304 Prominences. Astrophysical Journal Letters, 520, L71.

Wang, Y.M., & Sheeley, N.R., Jr. (2002). Observations of Core Fallback during Coronal Mass Ejections. Astrophysical Journal, 567, 1211.

Wang, Y.-M., & Muglach, K. (2007). On the Formation of Filament Channels. Astrophysical Journal, 666, 1284.

Yeates, A.R., Mackay, D.H., & van Ballegooijen, A.A. (2008). Modelling the Global Solar Corona II: Coronal Evolution and Filament Chirality Comparison. Solar Physics, 247, 103.

Zirin, H., & Severny, A. B. (1961). Measurement of magnetic fields in solar prominences. Observatory, 81, 155.8, 134.

Zirker, J.B., Engvold, O., & Yi, Z. (1994), Flows in quiescent prominences. Solar Physics, 150, 81.

Zirker, J.B., Engvold, O., & Martin, S.F. (1998). Counter-streaming gas flows in solar prominences as evidence for vertical magnetic fields. Nature, 396, 440.

## Further Reading

Arregui, I., Oliver, R., & Ballester, J.L. (2018). Prominence oscillations. Living Reviews in Solar Physics 15, 3.

Gibson, S.E. (2018). Solar prominences: theory and models. Living Reviews in Solar Physics 15, 7.

Labrosse, N., Heinzel, P., Vial, J.-C., Kucera, T., Parenti, S., Gunar, S., Schmieder, B., & Kilper, G. (2010). Physics of Solar Prominences: I Spectral Diagnostics and Non-LTE Modelling. Space Science Reviews, 151, 243.

Mackay, D.H., Karpen, J.T., Ballester, J.L., Schmieder, B., & Aulanier, G. (2010). Physics of Solar Prominences: II Magnetic Structure and Dynamics. Space Science Reviews, 151, 333.

Parenti, S. (2014). Solar Prominences: Observations. Living Reviews in Solar Physics 11, 1.

Priest, E.R. (2014). Magnetohydrodynamics of the Sun.

Tandberg-Hanssen, E. (2011). Solar Prominences – An Intriguing Phenomenon, Solar Physics, 269, 237.

Tandberg-Hanssen, E. (1995). The Nature of Solar prominences, Astrophysics and Space Science Library.

Vial, J.-C., & Engvold, O. (2015). Solar Prominences, 415.